SCIENCE CHINA
Information Sciences

• RESEARCH PAPER •

June 2016, Vol. 59 062308:1–062308:13
doi: 10.1007/s11432-016-5533-9

Robust and fast iterative sparse recovery method for space-time adaptive processing

Xiaopeng YANG*, Yuze SUN, Tao ZENG & Teng LONG

Beijing Key Laboratory of Embedded Real-time Information Processing Technology, School of Information and Electronics, Beijing Institute of Technology, Beijing 100081*, China*

Received June 20, 2015; accepted November 17, 2015; published online February 25, 2016

Abstract Conventional space-time adaptive processing (STAP) requires large numbers of independent and identically distributed (i.i.d) training samples to ensure the performance of clutter suppression, which is hard to be achieved in practical complex nonhomogeneous environment. In order to improve the performance of clutter suppression with small training sample support, a robust and fast iterative sparse recovery method for STAP is proposed in this paper. In the proposed method, the sparse recovery of clutter spatial-temporal spectrum and the calibration of space-time overcomplete dictionary are achieved iteratively. Firstly, the robust solution of sparse recovery is derived by regularized processing, which can be calculated recursively based on the block Hermitian matrix property, afterwards the mismatch of space-time overcomplete dictionary is calibrated by minimizing the cost function. The proposed method can not only alleviate the effect of noise and dictionary mismatch, but also reduce the computational cost caused by direct matrix inversion. Finally, the proposed method is verified based on the simulated and the actual airborne phased array radar data, which shows that the proposed method is suitable for practical complex nonhomogeneous environment and provides better performance compared with conventional STAP methods.

Keywords space-time adaptive processing (STAP), sparse recovery, robust, iteration, computational complexity

Citation Yang X P, Sun Y Z, Zeng T, et al. Robust and fast iterative sparse recovery method for space-time adaptive processing. Sci China Inf Sci, 2016, 59(6): 062308, doi: 10.1007/s11432-016-5533-9

1 Introduction

Space-time adaptive processing (STAP) is an effective technique to suppress clutter and achieve moving target detection for airborne phased array radar [1]. According to the RMB rule [1], full dimension STAP requires at least twice of the system degrees of freedom (DoFs) of the independent and identically distributed (i.i.d) training samples. However, in practical complex nonhomogeneous environment, it is very difficult to collect sufficient i.i.d training samples, so that the clutter suppression would severely deteriorate. So it is necessary to develop novel STAP methods which can achieve acceptable performance with small training sample requirement. In the past three decades, many STAP algorithms have been proposed to counteract this problem. Reduced-dimension STAP algorithms [2–5] such as the extended factored algorithm (EFA) and joint-domain localized (JDL) algorithm can reduce the requirement of

* Corresponding author (email: xiaopengyang@bit.edu.cn)

number of training samples to twice of the reduced-dimension. However, the performance of reduced-dimension STAP methods is easily influenced by the clutter environment. Reduced-rank STAP algorithms [6–8] such as the principle-components (PCs) and multistage Wiener filter (MWF) can reduce the number of training samples to twice of the clutter rank, but it is difficult to determine the rank of clutter in practical scenarios, and the inappropriate rank selection would lead to serious performance loss. Recently, knowledge-aided techniques have been developed to improve STAP performance with small training support. However, precise environmental prior knowledge is difficult to obtain effectively.

In recent years, the sparse recovery techniques have been applied for STAP. The sparse recovery techniques can effectively estimate the clutter spatial-temporal spectrum with limited training samples, which can significantly improve the convergence compared with conventional STAP methods. The problem of clutter spatial-temporal spectrum sparse recovery is usually formulated as basis pursuit de-noising (BPDN) problem [9–11], which can be solved by convex optimization. However, the computational complexity will increase extremely when the dimension of convex optimization becomes large, which is very difficult to be implemented for STAP. Focal underdetermined system solution (FOCUSS) employing l_p-norm minimization to achieve sparse recovery recursively [11] and the complex-valued Homotopy technique [12] have been investigated. However, the performance of these methods is heavily affected by the mismatch of the space-time overcomplete dictionary and additive noise. Moreover, the pseudo inverse operation in the recursive processing will lead to huge computational burden.

In order to improve the robustness of clutter suppression for noise and dictionary mismatch in practical complex nonhomogeneous environment and reduce the computational complexity caused by direct matrix inversion of conventional sparsity-based STAP methods, a robust and fast iterative sparse recovery method for STAP is proposed in this paper. In the proposed method, the sparse recovery of clutter spatial-temporal spectrum and the calibration of space-time overcomplete dictionary are executed iteratively. The robust solution of sparse recovery is derived by regularized processing and calculated recursively based on the block Hermitian matrix property, afterwards the mismatch of space-time overcomplete dictionary is calibrated by minimizing the cost function. The proposed method is verified based on simulated and actual airborne phased array radar data.

This paper is organized as follows. The signal model for side-looking airborne phased array radar is shown in Section 2. The sparsity of clutter spatial-temporal spectrum is analyzed in Section 3. The proposed robust and fast iterative sparse recovery method for STAP is derived in Section 4. The computational complexity is analyzed in Section 5. The clutter suppression performance is investigated based on the simulated data, MCARM data and actual measured airborne radar data in Section 6, and the conclusions are given in Section 7.

2 Signal model

The side-looking antenna array configuration of airborne phased array radar is considered, and the corresponding geometry is shown in Figure 1. The antenna array is composed of N antenna element linear array with uniform half-wavelength spacing, and aligned with the velocity direction of platform. M identical pulses are transmitted during each coherent processing interval (CPI) at a constant pulse repetition frequency (PRF) f_r. The platform altitude is h, the velocity is v_a, and the frequency wavelength is λ. It is known that radar detection is a binary hypothesis problem where hypothesis H_1 corresponds to target presence and hypothesis H_0 corresponds to target absence.

$$\begin{cases} H_0 : \boldsymbol{x} = \boldsymbol{x}_i, \\ H_1 : \boldsymbol{x} = \boldsymbol{x}_s + \boldsymbol{x}_i, \end{cases} \tag{1}$$

where x_i is composed of clutter x_c and noise x_n, x_s is the received target echo, and the space-time snapshot is expressed as a $NM \times 1$ vector.

The clutter data of each range cell can be modeled as the superposition of N_c independent clutter patches which are distributed in azimuth with angle interval $\Delta\varphi = 2\pi/N_c$. Each clutter patch can be

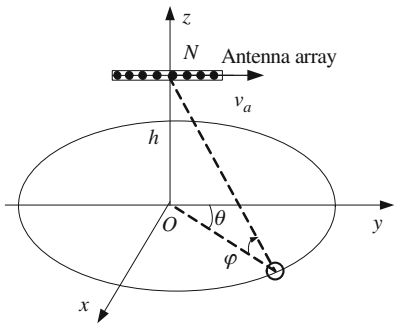

Figure 1 Geometry of side-looking antenna array configuration.

described by the elevation angle θ and the azimuth angle φ. The spatial frequency $\vartheta_{c,i}$ and the normalized Doppler frequency $\omega_{c,i}$ of the ith clutter patch can be respectively denoted by

$$\vartheta_{c,i} = \frac{d_A}{\lambda}\cos(\theta_i)\sin(\varphi_i), \qquad \omega_{c,i} = \frac{2v_a}{\lambda f_r}\cos(\theta_i)\sin(\varphi_i), \tag{2}$$

where $i = 1, 2, \ldots, N_c$, and d_A is the inter-element spacing. Hence the space-time steering vector of ith clutter patch can be expressed by

$$\boldsymbol{v}(\omega_{c,i}, \vartheta_{c,i}) = \boldsymbol{b}(\omega_{c,i}) \otimes \boldsymbol{a}(\vartheta_{c,i}), \tag{3}$$

where $\boldsymbol{b}(\omega_{c,i}) = [1, \exp(\mathrm{j}2\pi\omega_{c,i}), \ldots, \exp(\mathrm{j}(M-1)2\pi\omega_{c,i})]^{\mathrm{T}}$ is the $M \times 1$ temporal steering vector, and $\boldsymbol{a}(\vartheta_{c,i}) = [1, \exp(\mathrm{j}2\pi\vartheta_{c,i}), \ldots, \exp(\mathrm{j}(N-1)2\pi\vartheta_{c,i})]^{\mathrm{T}}$ is the $N \times 1$ spatial steering vector. $\otimes$ and $(\cdot)^{\mathrm{T}}$ denote the Kronecker product and vector transposition, respectively. The space-time clutter snapshot of lth range cell is expressed by

$$\boldsymbol{x}_c = \sum_{i=1}^{N_c} \tilde{\xi}_i \boldsymbol{v}_i, \tag{4}$$

where $\tilde{\xi}_i$ denotes the random complex amplitude corresponding to ith clutter patch associated with radar transmitting power, slant range, and antenna patterns. Thus, the space-time snapshot of lth range cell is

$$\boldsymbol{x}_l = \boldsymbol{x}_c + \boldsymbol{x}_n = \sum_{i=1}^{N_c} \tilde{\xi}_i \boldsymbol{v}(f_{s,i}, f_{d,i}) + \boldsymbol{x}_n, \tag{5}$$

where $\boldsymbol{x}_{t,l}(m)$ is the $N \times 1$ data vector received by mth pulse, and the noise is assumed to be Gaussian, spatially and temporally white. Hence the $NM \times NM$ space-time covariance matrix can be calculated by $\boldsymbol{R} = \mathrm{E}[\boldsymbol{x}_l \boldsymbol{x}_l^{\mathrm{H}}]$, where H is the conjugate transpose operator. The STAP weight vector is derived from the maximization of signal to clutter and noise ratio (SINR), which is given by

$$\boldsymbol{w} = \boldsymbol{R}^{-1} \boldsymbol{v}_t(\omega_t, \vartheta_t), \tag{6}$$

where $\boldsymbol{v}_t(\omega_t, \vartheta_t)$ is the target space-time vector, and $\boldsymbol{R}$ is a prior unknown in practice, which is usually estimated from training samples around the range cell under test as

$$\begin{aligned} \hat{R} &= \mathrm{E}[\boldsymbol{x}\boldsymbol{x}^{\mathrm{H}}] = \frac{1}{K-1} \sum_{k=1, k\neq l}^{K-1} \boldsymbol{x}_k \boldsymbol{x}_k^{\mathrm{H}} \\ &= \boldsymbol{R}_c + \sigma^2 \boldsymbol{I} = \sum\nolimits_{i=1}^{N_c} \mathrm{E}\left\{ \left| \tilde{\xi}_i \right|^2 \right\} \left[\boldsymbol{b}(f_{d,i}) \boldsymbol{b}(f_{d,i})^{\mathrm{H}} \right] \left[\boldsymbol{a}(f_{s,i}) \boldsymbol{a}(f_{s,i})^{\mathrm{H}} \right] + \sigma^2 \boldsymbol{I}, \end{aligned} \tag{7}$$

where K is the number of i.i.d training samples around lth range cell under test.

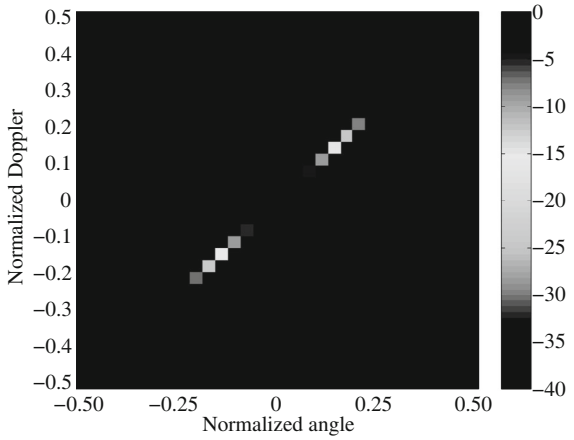

Figure 2 Sparse distribution of clutter spectrum in spatial-temporal plane.

3 Sparsity of clutter spatial-temporal spectrum

The clutter component $\boldsymbol{x}_c$ is the superposition of different clutter patches with corresponding spatial frequency and Doppler frequency as analyzed in Section 2. In order to demonstrate the sparsity of clutter spectrum, the whole spatial-temporal plane is firstly discretized into N_s and N_d, where $N_s = \rho_S N$ and $N_d = \rho_d M$ grids are the number of spatial and Doppler bins, respectively. Therefore Eq. (5) can be rewritten as

$$\boldsymbol{x}_l = \boldsymbol{x}_c + \boldsymbol{x}_n = \sum_{i=1}^{N_d}\sum_{j=1}^{N_s} \tilde{\gamma}_{i,j}\boldsymbol{v}\left(f_{d,i}, f_{s,j}\right) + \boldsymbol{x}_n = \boldsymbol{\Phi}\boldsymbol{\gamma}_l + \boldsymbol{x}_n, \tag{8}$$

where $\boldsymbol{\gamma}_l = [\tilde{\gamma}_{l,1,1}, \tilde{\gamma}_{l,1,2}, \ldots, \tilde{\gamma}_{l,N_s,N_d}]$ is the $N_sN_d \times 1$ complex amplitude of $\boldsymbol{x}_c$ from the lth range cell snapshot which represents the clutter spectrum. $NM \times N_sN_d$ matrix $\boldsymbol{\Phi}$ composed of all possible space-time steering vectors is the space-time overcomplete dictionary, which is given by

$$\boldsymbol{\Phi} = \left[\boldsymbol{v}\left(f_{d,1}, f_{s,1}\right), \boldsymbol{v}\left(f_{d,1}, f_{s,2}\right), \ldots, \boldsymbol{v}\left(f_{d,1}, f_{s,N_s}\right), \ldots, \boldsymbol{v}\left(f_{d,N_d}, f_{s,N_s}\right)\right]. \tag{9}$$

Then the space-time covariance matrix in (7) can be rewritten as

$$\boldsymbol{R} = \sum_{i=1}^{N_d}\sum_{j=1}^{N_s} \left|\tilde{\gamma}_{i,j}\right|^2 \boldsymbol{v}\left(f_{d,i}, f_{s,j}\right)\boldsymbol{v}\left(f_{d,i}, f_{s,j}\right)^{\mathrm{H}} + \sigma^2\boldsymbol{I}. \tag{10}$$

It is known that major components of the clutter spatial-temporal spectrum are distributed near the ridge determined by coupling relationship between the spatial frequency and the Doppler frequency of clutter. As shown in Figure 2, the complex amplitude in most area of the spatial-temporal plane is rather small, so the clutter spectrum shows great spares distribution character with respect to the whole plane. Therefore, if the complex amplitude $\boldsymbol{\gamma}_l$ can be estimated effectively based on the property of sparse distribution, the space-time covariance matrix $\boldsymbol{R}$ can be well reconstructed by complex amplitude and corresponding space-time steering vectors.

As N_sN_d is much bigger than the system DoFs, the space-time dictionary $\boldsymbol{\Phi}$ is overcomplete and highly correlated, so that Eq. (8) is undermined, which may have many solutions. However, based on the theory of sparse recovery [13–15], the ill-posed equation can be solved effectively with limited sample support. The sparse recovery of clutter spectrum can be formulated as BPDN problem, which is solved by the l_1-norm, and the minimization of l_1-norm is given as

$$\begin{aligned} &\hat{\boldsymbol{\gamma}}_l = \arg\ \min \left\|\boldsymbol{\gamma}_l\right\|_1 \\ &\text{subject to}\quad \left\|\boldsymbol{x}_l - \boldsymbol{\Phi}\boldsymbol{\gamma}_l\right\|_2 \leqslant \varepsilon, \end{aligned} \tag{11}$$

where l_1-norm guarantees the sparsity of $\boldsymbol{\gamma}_l$, and the l_2-norm restrains the estimation error within ε. Eq. (11) can also be given as LASSO problem

$$\hat{\boldsymbol{\gamma}}_l = \arg\min_{\boldsymbol{\gamma}_l} \left\{ \left\| \boldsymbol{x}_l - \boldsymbol{\Phi}\boldsymbol{\gamma}_l \right\|_2 + \kappa \left\| \boldsymbol{\gamma}_l \right\|_1 \right\}, \tag{12}$$

where κ is the regularization parameter. By averaging $\boldsymbol{\gamma}_l$ of each training sample, the sparse recovery of clutter spatial-temporal spectrum can be obtained, and then the space-time covariance matrix $\boldsymbol{R}$ and the adaptive weighting vectors will be implemented correspondingly.

4 Proposed robust and fast iterative sparse recovery method for STAP

The conventional sparsity-based STAP methods are generally developed by l_1-norm optimization, which has been shown in Section 3. However, the computational burden will become huge with the increase of the dimension of l_1-norm optimization, which restrains extremely the implementation of conventional sparsity-based STAP methods. FOCUSS method [16] is one of fast approximation algorithms, which has good sparse recovery performance for STAP based on l_p-norm optimization and iterative calculation [11]. However, the mismatch between the space-time overcomplete dictionary and actual clutter distribution is ignored in FOCUSS method, and the additive noise is also not considered in the iterations, so that the recovery performance of FOCUSS method will deteriorate significantly in practical complex nonhomogeneous environment. Moreover, the matrix inverse calculation is still considerable computational burden in the iterations.

In actual clutter environment, the clutter component would possibly be located between two grids rather than the exact gird point of the dictionary, so the mismatch between the space-time overcomplete and actual clutter distribution cannot be avoided. When the mismatch is considered, the space-time snapshot of lth range cell can be changed into [6]

$$\boldsymbol{x}_l = \boldsymbol{x}_c + \boldsymbol{x}_n = \sum_{i=1}^{N_d} \sum_{j=1}^{N_s} \tilde{\gamma}_{i,j} \boldsymbol{v}\left(f_{d,i}, f_{s,j}\right) + \boldsymbol{x}_n = \boldsymbol{\Theta}\boldsymbol{\gamma}_l + \boldsymbol{x}_n, \tag{13}$$

where $\boldsymbol{\Theta} = \boldsymbol{\Phi} + \boldsymbol{\Lambda}\boldsymbol{\Phi}$ denotes the actual overcomplete dictionary and $\boldsymbol{\Lambda}$ is the mismatch matrix. Therefore, a robust and fast iterative sparse recovery method for STAP in practical environment is proposed, and the main procedures of proposed method are mainly demonstrated in the following.

4.1 Sparse recovery processing

The effect of additive noise is not considered in the basic FOCUSS method [11]. However, the additive noise is invertible in practical environment, which will increase the recovery error of FOCUSS method. Therefore, in this paper the regularized processing is employed to reduce the effect of additive noise in the sparse recovery. So that the spares recovery problem in (11) can be converted as

$$\begin{aligned} &\min_{\boldsymbol{\gamma}_l} J\left(\boldsymbol{\gamma}_l\right) = \sum_{i=1}^{N_s N_d} \left\| \boldsymbol{\gamma}_{l,i} \right\|_p \\ &\text{subject to:} \quad \left\| \boldsymbol{x}_l - \boldsymbol{\Theta}\boldsymbol{\gamma}_l \right\|_2 \leqslant \varepsilon, \end{aligned} \tag{14}$$

then the cost function is given by Lagrange multiplier method

$$L\left(\boldsymbol{\gamma}_l\right) = J\left(\boldsymbol{\gamma}_l\right) + \alpha \left\| \boldsymbol{x}_l - \boldsymbol{\Theta}\boldsymbol{\gamma}_l \right\|_2, \tag{15}$$

where α is the Lagrange multipliers matching the noise level. By solving the gradient of $\boldsymbol{\gamma}_l$, we can get

$$\nabla L\left(\boldsymbol{\gamma}_l\right) = |p| \prod\left(\boldsymbol{\gamma}_l\right) \boldsymbol{\gamma}_l + \alpha \left(\boldsymbol{\Theta}^{\mathrm{H}}\boldsymbol{\Theta}\boldsymbol{\gamma}_l - \boldsymbol{\Theta}^{\mathrm{H}}\boldsymbol{x}_l \right), \tag{16}$$

where $\prod(\boldsymbol{\gamma}_l) = \mathrm{diag}(|\boldsymbol{\gamma}_{l,1}|^{p-2}, \ldots, |\boldsymbol{\gamma}_{l,N_sN_d}|^{p-2})$, then the appropriate Hessian matrix can be obtained by

$$\nabla^2 L\left(\boldsymbol{\gamma}_l\right) = |p| \prod\left(\boldsymbol{\gamma}_l\right) + \alpha \boldsymbol{\Theta}^{\mathrm{H}}\boldsymbol{\Theta}. \tag{17}$$

Afterwards by applying the quasi-Newton method, we can get

$$\boldsymbol{\gamma}_l^{(k+1)} = \boldsymbol{\gamma}_l^{(k)} - \left[\nabla^2 L\left(\boldsymbol{\gamma}_l^{(k+1)}\right)\right]^{-1} \cdot \nabla L\left(\boldsymbol{\gamma}_l^{(k+1)}\right). \tag{18}$$

Then by substituting (16) and (17) into (18), we can get

$$\boldsymbol{\gamma}_l^{(k+1)} = \left[\delta \prod\left(\boldsymbol{\gamma}_l^{(k)}\right) + \boldsymbol{\Theta}^{\mathrm{H}}\boldsymbol{\Theta}\right]^{-1} \boldsymbol{\Theta}^{\mathrm{H}}\boldsymbol{x}_l, \tag{19}$$

where $\delta = 1/\alpha$. By defining $(W^{(k)})^{-2} = \prod(\boldsymbol{\gamma}_l^{(k)})$ and $\boldsymbol{\Theta}^{(k)} = \boldsymbol{\Theta}W^{(k)}$, where

$$W^{(k)} = \mathrm{diag}\left(\left|\boldsymbol{\gamma}_{l,1}^{(k)}\right|^{1-p/2}, \ldots, \left|\boldsymbol{\gamma}_{l,N_sN_d}^{(k)}\right|^{1-p/2}\right)$$

is the diagonal weighting matrix at the kth iteration, and then the solution at kth iterative can be derived as

$$\boldsymbol{\gamma}_l^{(k+1)} = W^{(k)}\left(\boldsymbol{\Theta}^{(k)}\right)^{\mathrm{H}}\left[\delta I + \boldsymbol{\Theta}^{(k)}\left(\boldsymbol{\Theta}^{(k)}\right)^{\mathrm{H}}\right]^{-1}\boldsymbol{x}_l. \tag{20}$$

The low-resolution estimation based on Fourier spectrum is employed as the initial value of $\boldsymbol{\gamma}_l$, i.e., $\boldsymbol{\gamma}_l^{(0)} = \boldsymbol{\Phi}^{\mathrm{H}}\boldsymbol{x}_l$, and then the calculation can be executed iteratively as (20). During the iterations, the prominent components in $\boldsymbol{\gamma}_l^{(k)}$are gradually reinforced, while the remaining small components are suppressed until they become close to zero. Finally, when the absolute difference of $\boldsymbol{\gamma}_l^{(k)}$ is smaller than the convergence threshold, the spares recovery result is obtained. From (20), it can be found that when noise level is reduced to 0, i.e., $\delta \to 0$ the proposed method will degenerate to the FOCUSS method. Because the regularized processing is applied in the iteration, the proposed method can effectively improve the recovery performance under noise.

It is easily found from (20) that the matrix inversion is still needed to calculate complex amplitude, which will significantly influence the convergence of iteration. Although the adaptive subspace selection [11] can be applied to reduce the dimension of complex amplitude in the iterations, the direct inverse calculation still cannot be avoided. However, based on the mathematical analysis, it can be proved that the matrix $\boldsymbol{T} = \delta\boldsymbol{I} + \boldsymbol{\Theta}^{(k)}(\boldsymbol{\Theta}^{(k)})^{\mathrm{H}}$ is a Hermitian matrix, therefore the matrix inversion can be calculated recursively based on the block Hermitian matrix property [17–19]. Assuming that $\boldsymbol{T}$ is the $D \times D$ matrix, $\boldsymbol{T}_{d+1}$ is the $(d+1)$th leading principal minor of $\boldsymbol{T}$, i.e., $\boldsymbol{T}_{d+1} = \boldsymbol{T}(1:d+1, 1:d+1)$, where $d = 1, 2, \ldots, D-1$. The inverse matrix of $\boldsymbol{T}_{d+1}$ can be calculated by the inverse matrix of dth leading principal minor $\boldsymbol{T}_d$, and defined as $\boldsymbol{Q}_{d+1}$, which is also a Hermitian matrix

$$\boldsymbol{Q}_{d+1} = \begin{bmatrix} \boldsymbol{Q}_d & \boldsymbol{q}_{d+1} \\ \boldsymbol{q}_{d+1}^{\mathrm{H}} & q_{d+1} \end{bmatrix}, \tag{21}$$

where q_{d+1} is the $(d+1)$th diagonal component of $\boldsymbol{Q}_{d+1}$, i.e., $q_{d+1} = \boldsymbol{Q}_{d+1}(d+1, d+1)$. $\boldsymbol{q}_{d+1}$ is the column vector consisting of the first d components of $\boldsymbol{Q}_{d+1}$, i.e., $\boldsymbol{q}_{d+1} = \boldsymbol{Q}_{d+1}(1:d, 1:d)$. $\boldsymbol{Q}_d = \boldsymbol{Q}_{d+1}(1:d, 1:d)$ denotes the dth leading principal minors of $\boldsymbol{Q}_{d+1}$. Based on mutual inverse principle, $\boldsymbol{T}_{d+1}\boldsymbol{Q}_{d+1}$ can be calculated as

$$\boldsymbol{T}_{d+1}\boldsymbol{Q}_{d+1} = \begin{bmatrix} \boldsymbol{T}_d & \boldsymbol{t}_{d+1} \\ \boldsymbol{t}_{d+1}^{\mathrm{H}} & t_{d+1} \end{bmatrix}\begin{bmatrix} \boldsymbol{Q}_d & \boldsymbol{q}_{d+1} \\ \boldsymbol{q}_{d+1}^{\mathrm{H}} & q_{d+1} \end{bmatrix} = \begin{bmatrix} \boldsymbol{I}_d & \boldsymbol{0}_{d+1} \\ \boldsymbol{0}_{d+1}^{\mathrm{H}} & 1 \end{bmatrix}, \tag{22}$$

where $t_{d+1} = \boldsymbol{T}_{d+1}(d+1, d+1)$, and $\boldsymbol{0}_{d+1}$ is $d \times 1$ zero vector. Thus, the inverse matrix of $\boldsymbol{T}_{d+1}$ can be obtained by

$$\boldsymbol{T}_{d+1}^{-1} = \begin{bmatrix} \boldsymbol{T}_d^{-1} & \boldsymbol{0}_{d+1} \\ \boldsymbol{0}_{d+1}^{\mathrm{H}} & 0 \end{bmatrix} + \frac{1}{\alpha_{d+1}}\begin{bmatrix} \boldsymbol{b}_{d+1}\boldsymbol{b}_{d+1}^{\mathrm{H}} & \boldsymbol{b}_{d+1} \\ \boldsymbol{b}_{d+1}^{\mathrm{H}} & 1 \end{bmatrix}, \tag{23}$$

where $\boldsymbol{b}_{d+1} = -\boldsymbol{T}_d^{-1}\boldsymbol{t}_{d+1}$, $\alpha_{d+1} = t_{d+1} - \boldsymbol{t}_{d+1}^{\mathrm{H}}\boldsymbol{T}_d^{-1}\boldsymbol{t}_{d+1} = t_{d+1} + \boldsymbol{t}_{d+1}^{\mathrm{H}}\boldsymbol{b}_{d+1}$. According to (23), it is found that the inverse matrix can be obtained recursively by the leading principal minor of $\boldsymbol{T}$, which avoids calculating the inverse matrix directly in the iteration.

4.2 Mismatch calibration processing

The mismatch between the space-time overcomplete dictionary and actual clutter distribution is ignored in conventional sparsity-based STAP methods, which would decrease the performance of clutter suppression. Therefore, the mismatch calibration processing is investigated in this paper. After $\gamma_l^{(k)}$ is obtained at the kth iteration, the estimation of $\boldsymbol{\Lambda}$ can be obatined by

$$\boldsymbol{\Lambda}^{(k)} = \arg\min_{\boldsymbol{\Lambda}^{(k)}} J\left(\boldsymbol{\Lambda}^{(k)}\right) = \left\|\boldsymbol{\Lambda}^{(k)}\boldsymbol{\Phi}\right\|_2 + \left\|\boldsymbol{x}_l - \boldsymbol{\Theta}^{(k)}\boldsymbol{\gamma}_l^{(k)}\right\|_2. \tag{24}$$

By defining $\boldsymbol{e}^{(k)} = \boldsymbol{x}_l - \boldsymbol{\Phi}\boldsymbol{\gamma}_l^{(k)}$, and $\boldsymbol{y}^{(k)} = \boldsymbol{\Phi}\boldsymbol{\gamma}_l^{(k)}$, the cost function of (24) can be given as

$$J\left(\boldsymbol{\Lambda}^{(k)}\right) = \left\|\boldsymbol{\Lambda}^{(k)}\boldsymbol{\Phi}\right\|_2 + \left\|\boldsymbol{e}^{(k)} - \boldsymbol{\Lambda}^{(k)}\boldsymbol{y}^{(k)}\right\|_2. \tag{25}$$

Then the mismatch can be calculated by solving gradient equation

$$\frac{\partial J\left(\boldsymbol{\Lambda}^{(k)}\right)}{\partial \boldsymbol{\Lambda}^{(k)}} = \boldsymbol{\Lambda}^{(k)}\left(\boldsymbol{\Phi}\boldsymbol{\Phi}^{\mathrm{H}} + \boldsymbol{y}^{(k)}\left(\boldsymbol{y}^{(k)}\right)^{\mathrm{H}}\right) - \boldsymbol{e}^{(k)}\left(\boldsymbol{y}^{(k)}\right)^{\mathrm{H}} = 0. \tag{26}$$

Therefore the estimation of $\boldsymbol{\Lambda}$ can be obtained

$$\boldsymbol{\Lambda}^{(k)} = \boldsymbol{e}^{(k)}\left(\boldsymbol{y}^{(k)}\right)^{\mathrm{H}}\left(\boldsymbol{y}^{(k)}\left(\boldsymbol{y}^{(k)}\right)^{\mathrm{H}} + \boldsymbol{\Theta}\boldsymbol{\Theta}^{\mathrm{H}}\right)^{-1}. \tag{27}$$

Afterwards, the space-time overcomplete dictionary is calibrated at the kth iteration by $\boldsymbol{\Theta}^{(k)} = \boldsymbol{\Phi} + \boldsymbol{\Lambda}^{(k)}\boldsymbol{\Phi}$. It can be found that the mismatch of space-time overcomplete dictionary can be calibrated gradually by minimizing the corresponding cost function, so that the mismatch between the dictionary and actual clutter distribution has been reduced effectively.

When the following convergence condition is satisfied as

$$\left|\frac{\boldsymbol{\gamma}_l^{(k+1)} - \boldsymbol{\gamma}_l^{(k)}}{\boldsymbol{\gamma}_l^{(k+1)}}\right| \leqslant \xi, \tag{28}$$

the iteration will stop, and then the sparse recovery is achieved. Then the reconstruction of space-time covariance matrix $\boldsymbol{R}$ and adaptive weighting vector can be calculated correspondingly. The overall implementation diagram of proposed method is summarized in Figure 3.

5 Computational complexity analysis

In this section, the computational complexity of the proposed method is analyzed and compared with conventional STAP methods such as the sample matrix inversion (SMI) method, the disciplined convex programming (CVX) method and the FOCUSS method. It is assumed that the system DoFs is D_{DoFs}, L_{SMI} is the number of training samples for SMI method, L_{SP} is the number of training samples for CVX method, FOCUSS method and the proposed method, ρ_S and ρ_d are the resolution scale of spatial and Doppler axis, respectively. K_{FOCUSS} and K_{PRO} are the numbers of iteration of FOCUSS and proposed method, respectively. Then the computational complexity of SMI, CVX, FOCUSS and proposed methods is summarized in Table 1.

In order to understand the computational complexity intuitively, the simulations have been carried out and the corresponding results are shown in Figure 4. In the simulations, the number of DoFs D ranges from 16 to 256, L_{SMI} is $2D_{\mathrm{DoFs}}$ and L_{SP} is 8, the resolution scale ρ_S and ρ_d are 4, respectively, all the results are averaged over 500 Monte Carlo simulations.

It can be found from Table 1 and Figure 4 that the computational complexity of CVX method is higher than that of other sparsity-based methods. The computational complexity of FOCUSS and proposed method are decided by the size of iterations, which can be effectively reduced by adaptive subspace selection. However, compared with FOCUSS method, the direct matrix inversion is avoided by recursive

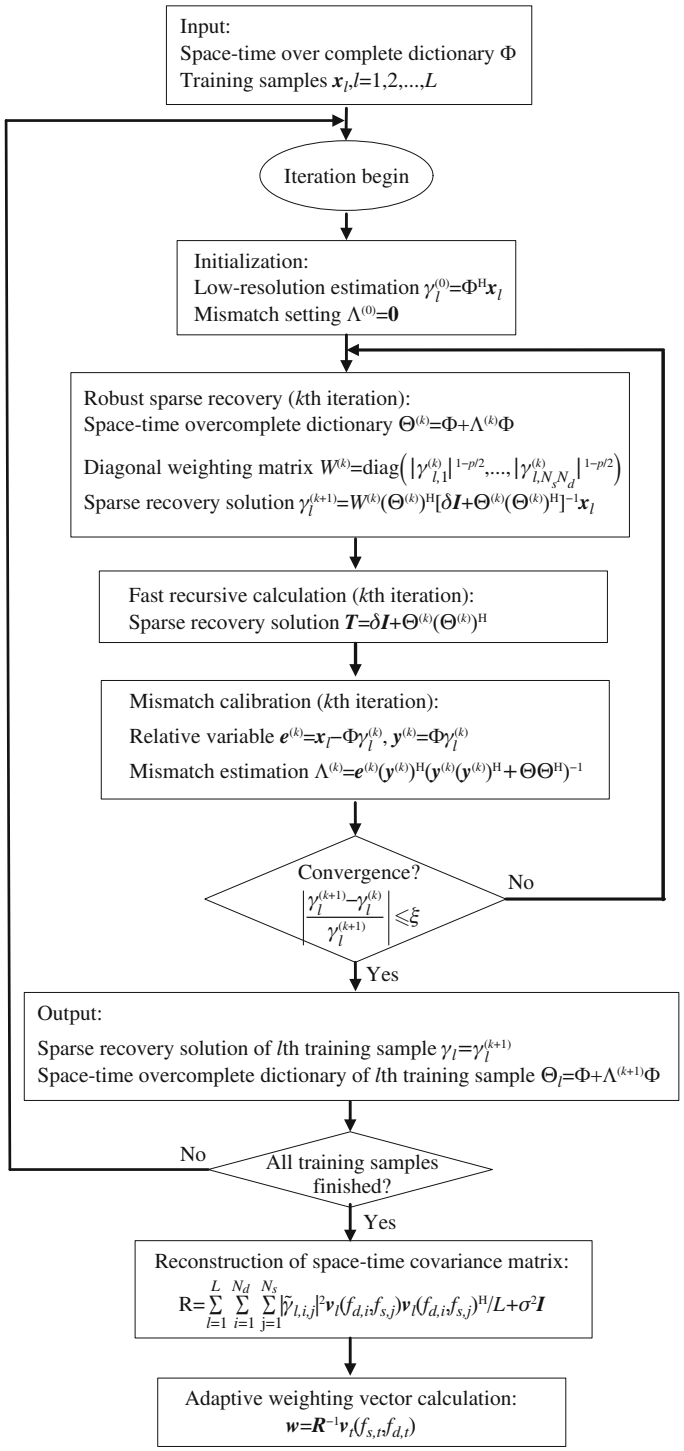

Figure 3 Overall implementation diagram of the proposed method.

calculation in the proposed method. Moreover, owing to the robust sparse recovery, the number of iteration can also be reduced, so the proposed method can effectively reduce the computational cost. When the number of DoFs is 128, the computational complexity of FOCUSS method and the proposed method are 6.664×10^4 MFLOPs and 1.319×10^4 MFLOPs, it is found that the computational complexity of the proposed method is reduced by 80%. Meanwhile, although SMI method can provide much lower computational complexity than sparsity-based methods, it should be noticed that SMI method requires much more number of training samples. If and only if L_{SMI} is at least twice of the DoFs, SMI method can

Table 1 Computational complexity of SMI, CVX, FOCUSS and proposed method

Method	Computational complexity
SMI	$O\left(L_{\mathrm{SMI}}\left(D_{\mathrm{DoFs}}\right)^2+D_{\mathrm{DoFs}}^3\right)$
CVX	$O\left(L_{\mathrm{SP}}\sum_{i=1}^{K_{\mathrm{Focuss}}}\left(\rho_s\rho_d D_{\mathrm{DoFs}}\right)^3+D_{\mathrm{DoFs}}^3\right)$
FOCUSS	$O\left(L_{\mathrm{SP}}\sum_{i=1}^{K_{\mathrm{Focuss}}}\left(K_{\mathrm{Focuss},i}\right)^3+D_{\mathrm{DoFs}}^3\right)$
Proposed method	$O\left(L_{\mathrm{SP}}\sum_{i=1}^{K_{\mathrm{PRO}}}2\left(K_{\mathrm{Focuss},i}\right)^3/3+D_{\mathrm{DoFs}}^3\right)$

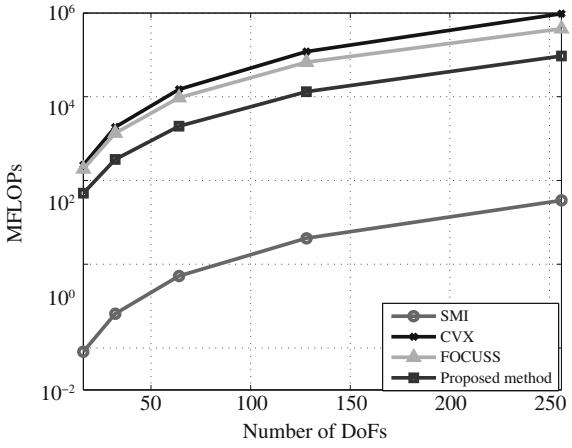

Figure 4 Computational complexity of SMI, CVX, FOCUSS and proposed method, when D_{DoFs} ranges from 16 to 256.

Table 2 Simulation parameters

Parameter	Value	Parameter	Value
Number of spatial elements	8	Number of temporal pulses in a CPI	8
Radar frequency	450 MHz	Pulse repetition frequency	1200 Hz
Platform velocity	200 m/s	Height of platform	12 km
Main beam look direction	side-looking	Clutter-to-noise ratio (CNR)	40 dB
Target normalized Doppler frequency	0.15	SNR	5 dB

just obtain the acceptable performance. However, so many training samples are very difficult to collect in practical complex nonhomogeneous environment. On the other hand, the sparsity-based methods can provide much better performance than SMI method, even the number of training samples is very small, such as only 4–8 available training samples.

6 Clutter suppression performance analysis

In this section, simulated data, MCARM data [20] and actual measured airborne phased array radar data are used to verify the clutter suppression performance of the proposed methods, and compared with SMI, EFA, CVX, and FOCUSS methods.

6.1 Simulated data

The simulation parameters are listed in Table 2, where ρ_S and ρ_d are 4, respectively, and all the results are averaged over 500 Monte Carlo runs.

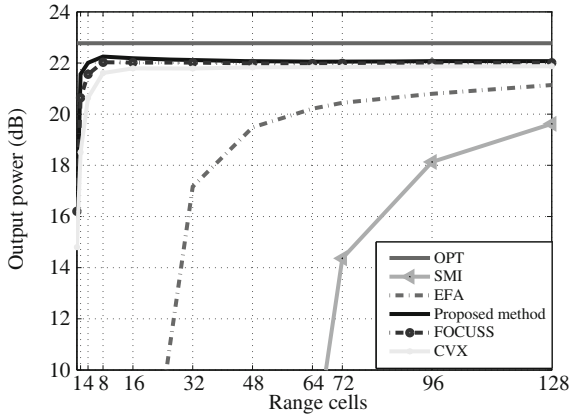

Figure 5 Output SINRs versus number of snapshots.

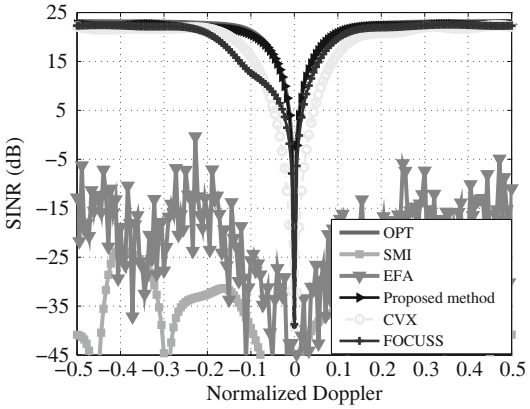

Figure 6 Output SINRs of SMI, EFA, CVX, FOCUSS and proposed method.

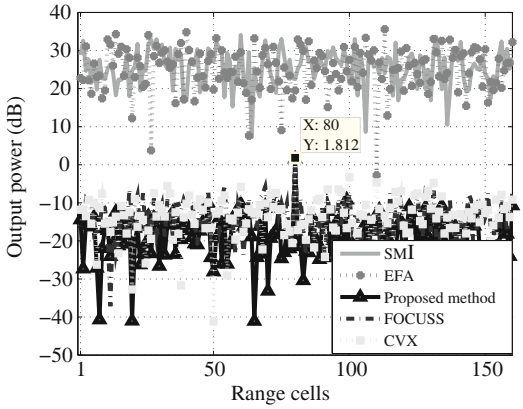

Figure 7 Range detections of SMI, EFA, CVX, FOCUSS and proposed method.

The output SINRs versus the number of snapshots based on SMI, EFA, CVX, FOCUSS and the proposed method are investigated and the results are shown in Figure 5. It is found that the sparsity-based STAP methods can obtain desirable SINR performance with small training sample support, which exhibits much faster convergence than conventional STAP methods. Meanwhile, the proposed method can provide better performance than other sparsity-based methods with the same number of training samples, because the calibration of space-time overcomplete dictionary and the regularization in the sparse recovery processing are applied in the proposed method.

The output SINRs with 4 training samples are investigated correspondingly and the results are shown in Figure 6. It is found that SMI and EFA methods cannot obtain desirable SINR with small training sample support, owing to the insufficient estimation of clutter covariance matrix, so that these two methods could not provide desirable target detection performance in practical clutter environment. However, the sparsity-based STAP methods could provide much better performance, because of good estimation of clutter distribution so that the clutter covariance matrix can be well reconstructed. Moreover, the proposed method can obtain better sparse recovery performance than conventional sparsity-based STAP methods because of the calibration of space-time overcomplete dictionary and regularization processing. The proposed method can effectively improve the SINR performance, especially in low Doppler frequency region where the target is located.

In the following, the range detections with 4 training samples are also investigated correspondingly and the results are shown in Figure 7. It is also found that SMI and EFA methods cannot suppress the clutter effectively with small training sample support, owing to the insufficient estimation of clutter covariance matrix, so that these two methods could not provide desirable target detection performance in practical clutter environment. However, the sparsity-based STAP methods can effectively suppress the

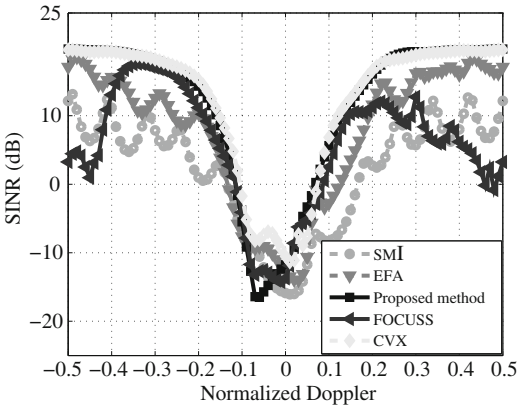

Figure 8 Output SINRs of SMI, CVX, FOCUSS and proposed method based on MCARM data.

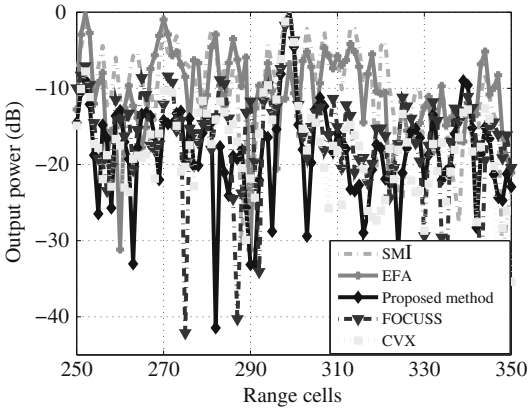

Figure 9 Range detections of SMI, EFA, CVX, FOCUSS and proposed method based on MCARM data.

clutter, because of good reconstruction of clutter covariance matrix. Moreover, the proposed method can obtain better range detection performance than conventional sparsity-based STAP methods, because the proposed method can produce the larger difference of output power between tested range cell and adjacent range cells than FOCUSS and CVX methods, which is in accordance with results shown in Figure 6. The proposed method will be very useful for target detection in practical complex nonhomogeneous environment.

6.2 MCARM data

The MCARM data [20] is used to verify the STAP methods in this section, the selected data is from acquisition 575 on flight 5 (file RL050575). The array was an L-band phased array antenna using 22 elements arranged as 2×11 configuration. The PRF of the radar is 1984 Hz, 128 pulses are contained in one CPI, the platform velocity is 100 m/s, and the height of the platform is 3078 m. ρ_S and ρ_d are set to 6 respectively. 12 pulses and 8 elements data of MCARM are used, the target is located at the 299th range cell with -0.15 Doppler frequency, 4 range cell data around the 299th range cell are selected as the training samples.

The output SINRs are investigated and the results are shown in Figure 8. It is similar with the previous simulated results that SMI and EFA methods cannot obtain desirable SINR with small training sample support. Moreover, the proposed method can obtain better SINR performance in both main-lobe and side-lobe regions than conventional sparsity-based STAP methods.

The range detections are also investigated and the results are shown in Figure 9. It is similar with the previous simulated results that SMI and EFA methods cannot detect target effectively, while the sparsity-based STAP methods can provide desirable detection. The proposed method can also obtain larger difference of the output power between tested range cell and adjacent range cells than FOCUSS and CVX methods, so that the target can be detected correctly.

6.3 Actual measured airborne radar data

Some actual measured airborne radar data is also applied to verify the proposed method compared with SMI, EFA, CVX, FOCUSS methods in the section. The actual measured airborne radar data consists of 16 spatial channels and 128 temporal pulses in a CPI. ρ_S and ρ_d are set to 6, respectively and 100 range snapshots of the first 8 channels and the first 12 pulses are used, a strong target is located in the 231st range cell with the normalized Doppler about 0.07, 4 range cell data around the 231st range cell are selected as the training samples.

The output SINRs are also investigated and the results are shown in Figure 10. It is similar with the previous results based on simulated data and MCARM data that SMI and EFA methods cannot obtain

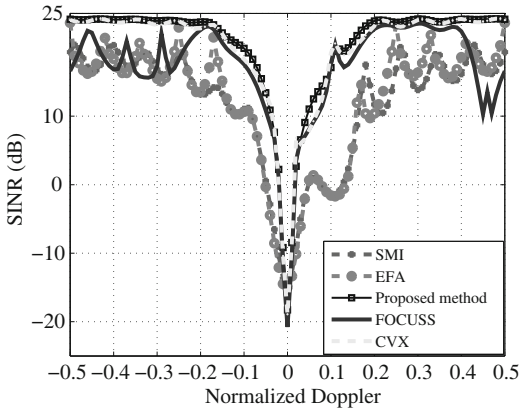

Figure 10 Output SINRs of SMI, CVX, FOCUSS and proposed method based on actual measured airborne radar data.

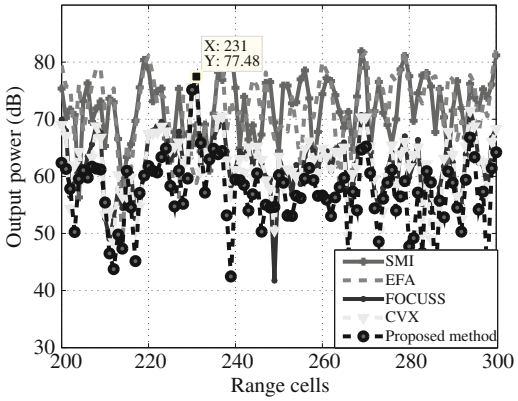

Figure 11 Range detections of SMI, EFA, CVX, FOCUSS and proposed method based on actual measured airborne radar data.

desirable SINR, while the sparsity-based STAP methods provide better performance with limited training samples, and the proposed method can obtain better performance especially in main-lobe region.

The range detection results are shown in Figure 11. It is also similar with the previous results based on simulated data and MCARM data that SMI and EFA methods cannot detect target effectively, while the sparsity-based STAP methods can provide desirable detection, and the proposed method can obtain larger difference of the output power between tested range cell and adjacent range cells than FOCUSS and CVX methods.

7 Conclusion

In this paper, a robust and fast iterative sparse recovery method for STAP has been proposed for practical complex nonhomogeneous environment. In the proposed method, the sparse recovery of clutter spatial-temporal spectrum and the calibration of space-time overcomplete dictionary are achieved iteratively. Firstly by regularized processing, the robust solution of sparse recovery is derived and calculated recursively based on the block Hermitian matrix property, afterwards the mismatch of space-time overcomplete dictionary is calibrated by minimizing the cost function. The proposed method can not only alleviate the effect of noise and dictionary mismatch, but also reduce the computational cost caused by direct matrix inversion. Based on the simulated and the actual airborne phased array radar data, it has been verified that the proposed method is suitable for practical complex nonhomogeneous environment and provide better performance compared with conventional STAP methods.

Acknowledgements This work was supported by 111 Project of China (Grant No. B14010) and National Natural Science Foundation of China (Grant Nos. 61225005, 61120106004).

Conflict of interest The authors declare that they have no conflict of interest.

References

1 Reed I S, Mallet J D, Brennan L E. Rapid convergence rate in adaptive arrays. IEEE Trans Aerosp Electron Syst, 1974, 10: 853–863
2 Wang Y L, Peng Y N, Bao Z. Space-time adaptive processing for airborne radar with various array orientation. IET Radar Sonar Navig, 1997, 144: 330–340
3 Zhang W, He Z, Li J. A method for finding best channels in beam-space post-Doppler reduced-dimension STAP. IEEE Trans Aerosp Electron Syst, 2013, 50: 254–264
4 Wang H, Cai L. On adaptive spatial-temporal processing for airborne surveillance radar systems. IEEE Trans Aerosp Electron Syst, 1994, 30: 660–670
5 Long T, Liu Y X, Yang X P. Improved eigenanalysis canceler based on data-independent clutter subspace estimation for space-time adaptive processing. Sci China Inf Sci, 2013, 56: 102301

6 Fa R, de Lamare R C. Reduced rank STAP algorithms using joint iterative optimization of filters. IEEE Trans Aerosp Electron Syst, 2011, 47: 1668–1684
7 Wang Y L, Liu W J, Xie W C. Reduced-rank space-time adaptive detector for airborne radar. Sci China Inf Sci, 2014, 57: 082310
8 Liu W J, Xie W C, Wang Y L. Adaptive detectors in the Krylov subspace. Sci China Inf Sci, 2014, 57: 102310
9 Selesnick I W, Pillai S U, Li K Y, et al. Angle-Doppler processing using sparse regularization. In: Proceedings of IEEE International Conference on Acoustics, Speech and Signal Processing, Dallas, 2010. 2750–2753
10 Wang W W, Liao G S, Zhu S Q. Compressive sensing-based ground moving target indication for dual-channel synthetic aperture radar. IET Radar Sonar Navig, 2013, 7: 858–866
11 Sun K, Meng H D, Wang Y L, et al. Direct data domain STAP using sparse representation of clutter spectrum. Signal Process, 2011, 91: 2222–2236
12 Yang Z C, Li X, Wang H Q, et al. Sparsity-based space-time adaptive processing using complex-valued homotopy technique for airborne radar. IET Signal Process, 2014, 8: 552–564
13 Donoho D L, Elad M, Temlyakov V N. Stable recovery of sparse overcomplete representations in the presence of noise. IEEE Trans Inf Theory, 2006, 52: 6–18
14 Candes E, Romberg J, Tao T. Stable signal recovery from incomplete and inaccurate measurements. Commun Pure Appl Math, 2006, 59: 1207–1223
15 Jia Q Q, Wu R B. Space time adaptive parameter estimation of moving target based on compressed sensing. J Electron Inf Technol, 2013, 35: 2714–2720
16 Rao B D, Engan K, Cotter S F, et al. Subset selection in noise based on diversity measure minimization. IEEE Trans Signal Process, 2003, 51: 760–770
17 Gao F, Wang Y L, Chen H. Study on matrix inversion for STAP. Radar Sci Technol, 2008, 6: 215–218
18 Yang X P, Liu Y X, Long T. A pulse-order recursive method for inverse covariance matrix computation applied to space-time adaptive processing. Sci China Inf Sci, 2013, 56: 042312
19 Yang X P, Sun Y Z, Liu Y X, et al. Fast inverse covariance matrix computation based on element-order recursive method for space-time adaptive processing. Sci China Inf Sci, 2015, 58: 022304
20 Babu B N S, Torres J A, Melvin W L. Processing and evaluation of multichannel airborne radar measurements (M-CARM) measured data. In: Proceedings of IEEE International Symposium on Phased Array Systems and Technology, Boston, 1996. 395–399